FERMILAB-CONF-09-656-CMS

Inclusive W/Z Production at CMS

P. Tan *on behalf of the CMS Collaboration*
Fermi National Accelerator Laboratory, P.O. Box 500, Batavia, IL 60510, USA

At the LHC, the production cross sections of W/Z bosons are tens to hundreds of nanobarns. The production mechanism of these processes is well established in the Standard Model and these processes can be used as "standard candles" to help commission the CMS detector for physics. Leptonic decays of W/Z bosons are expected to have very high trigger efficiency and signal to background ratio. Therefore they are ideal channels to study the properties of W/Z bosons in detail, such as cross sections and charge asymmetry. In this paper early CMS results on inclusive W/Z production at 10 TeV center-of-mass energy are discussed.

1. Introduction

The W and Z bosons were first discovered at CERN more than two decades ago [1, 2]. Since then their properties have been extensively studied by different experiments to test the Standard Model (SM) predictions and to explore the physics beyond-the-SM. At the Large Hadron Collider (LHC) [3], W and Z bosons will be produced with large rates. A large set of W/Z bosons will help us with detector commissioning initially and enable us to perform a large variety of W/Z physics studies with early LHC data.

The production mechanism of W/Z bosons at the LHC is well known. Higher order predictions of many W/Z observables have been carried out. For example, a recent next-to-leading order calculation [4] of total W and Z cross sections predicted that the cross sections are tens to hundreds of nanobarns for Z and W bosons, respectively. A calculation of differential cross section as a function of boson rapidity at next-to-next-leading order has also been carried out by C. Anastasiou *et al.* [5]. In these theoretical predictions, errors due to the Parton Distribution Functions (PDF) dominated total theoretical errors. The PDF error could be partially canceled out if we study ratios of cross sections, such as the lepton charge asymmetry between W^+ and W^- production, which is defined to be,

$$A(\eta) = \frac{\frac{d\sigma}{d\eta}(W^+ \to l\nu) - \frac{d\sigma}{d\eta}(W^- \to l\nu)}{\frac{d\sigma}{d\eta}(W^+ \to l\nu) + \frac{d\sigma}{d\eta}(W^- \to l\nu)}. \quad (1)$$

This charge asymmetry probes the valence-sea quark ratio in protons. Measurements of these observables at the LHC will enable us to test higher order calculations and provide new insights into proton structure.

2. CMS Detector

The Compact Muon Solenoid (CMS) experiment is a 4π general-purpose hadron-collider detector, which is suitable for high-p_T physics studies at the LHC. The central feature of the Compact Muon Solenoid apparatus is a superconducting solenoid, of 6 m internal diameter, providing a field of 3.8 T. Within the field volume are the silicon pixel and strip tracker, the crystal electromagnetic calorimeter (ECAL) and the brass/scintillator hadronic calorimeter (HCAL). Muons are measured in gaseous detectors embedded in the iron return yoke. Besides the barrel and endcap detectors, CMS has extensive forward calorimetry. The ECAL has an energy resolution of better than 0.5 % above 100 GeV. The HCAL, when combined with the ECAL, measures jets with a resolution $\Delta E/E \approx 100\,\%/\sqrt{E} \oplus 5\,\%$. The calorimeter cells are grouped in projective towers, of granularity $\Delta\eta \times \Delta\phi = 0.087 \times 0.087$ at central rapidities and 0.175×0.175 at forward rapidities. The muons are measured in the pseudorapidity window $|\eta| < 2.4$, with detection planes made of three technologies: Drift Tubes, Cathode Strip Chambers, and Resistive Plate Chambers. Matching the muons to the tracks measured in the silicon tracker results in a transverse momentum resolution between 1 and 5 %, for p_{T} values up to 1 TeV/c. The first level of the CMS trigger system, composed of custom hardware processors, uses information from the calorimeters and muon detectors to select (in less than 1 μs) the most interesting events (only one bunch crossing in 1000). The High Level Trigger processor farm further decreases the event rate from 100 kHz to 100 Hz, before data storage. A much more detailed description of CMS can be found elsewhere [6].

3. Event Simulation

The Monte Carlo (MC) simulation used in the following studies was generated with the Pythia [7] event generator, where the CTEQ5L [8] PDF model was used. The center-of-mass energy was assumed to be 10 TeV. The generated events were then passed through the full CMS detector simulation with GEANT4 [9]. Physics objects such as muons and electrons were reconstructed with standard CMS offline reconstruction sequence. The missing transverse energy (MET) was reconstructed using energy deposits in CMS calorimeters.

4. Inclusive W Boson Cross Section

At the LHC, leptonic decays of W/Z bosons were used to study the properties of W/Z bosons. The experimental signature of a W boson is a high-p_T lepton and large MET due to presence of a neutrino in the final state. CMS conducted analyses to measure the inclusive W boson cross section in both muon and electron decays [10, 11].

The trigger used in $W \to \mu\nu$ analysis is a single muon trigger with a minimum p_T threshold of 15 GeV. The efficiency is above 90%. The CMS single muon trigger system has coverage up to a pseudorapidity of $|\eta| < 2.1$. The selection of $W \to \mu\nu$ candidates was done by first requiring an isolated muon with $p_T >$ 25 GeV and muon pseudorapidity $|\eta|$ <2.0. Here the isolation is the p_T sum of all tracks in a cone of radius 0.3 around the muon direction, normalized to the muon p_T. This normalized isolation is required to be less than 0.09. The QCD dijet background was largely suppressed by the isolation requirement. Other processes, such as Drell-Yan, $t\bar{t}$, $W \to \tau\nu$, could also fake a $W \to \mu\nu$ event. Background events were further suppressed by requiring transverse mass [1] $m_T > 50$ GeV, as shown in Fig. 1, where the expected $W \to \mu\nu$ signal and background events for an integrated luminosity of 10 pb^{-1} is shown.

CMS also studied the inclusive W boson cross section in electron decays. A single electron trigger was used, which has an efficiency of about 97%. An electron candidate was required to have transverse energy (E_T) deposit in the CMS ECAL detector $E_T >$ 30 GeV and $|\eta|$ <2.5. The shower shape of a electron candidate was also required to be consistent with an electromagnetic interaction. Comparing to the muon channel analysis, in addition to background processes such as, QCD dijet production, Drell-Yan, $t\bar{t}$, $W \to \tau\nu$, photon plus jet production also contributes. The QCD dijet background was significantly reduced by an isolation requirement. Here isolation was computed using transverse components of energy deposits in CMS calorimeters and tracks in a cone of radius 0.4 around the electron direction. Figure 1 shows the reconstructed MET distribution for $W \to e\nu$ signal and background events after all event selections were applied.

The $W \to l\nu$ cross section is related to the background subtracted number of signal events, N_W,

$$\sigma_W \times BR(W \to l\nu) = \frac{N_W}{A_W \times \epsilon_W \times \mathcal{L}}, \qquad (2)$$

[1] Here $m_T = \sqrt{2 \cdot p_T \cdot MET \cdot (1 - cos(\Delta\phi_{\mu,MET}))}$, where $\Delta\phi_{\mu,MET}$ is the angular difference between muon and missing transverse moment in the plane transverse to the beam direction.

where A_W is acceptance for W signal events, ϵ_W is the W reconstruction and selection efficiency, and $\mathcal{L}$ is the integrated luminosity. While acceptance has to be estimated with MC, the lepton reconstruction and selection efficiency can be derived directly from data with a tag-and-probe method [12]. The expected statistical error of the measured cross section is 1.5% for an integrated luminosity of 10 pb^{-1}. The systematic error is expected to be dominated by the luminosity error, which is expected to be about 10% at the CMS start-up [13].

5. Inclusive Z Boson Cross Section

Similarly the inclusive Z boson production is another "standard candle" to help us commision CMS for physics. CMS studied experimental sensitivities to the inclusive Z boson cross section in both di-muon and di-electron decays [10, 11]. Comparing to the $W \to l\nu$ analysis, due to presence of two isolated high-p_T leptons the background was expected to be less than one percent after final event selection. The major background contributions were from QCD dijet, W plus jets, $t\bar{t}$, $Z \to \tau\tau$. Figure 2 shows the reconstructed $Z \to ee$ invariant mass distribution for an integrated luminosity of 10 pb^{-1}. Both expected signal and background contributions are shown. The final $Z \to ee$ sample was selected from events with 70 GeV $< m_{ee} <$110 GeV. The cross sections were obtained after correcting for efficiencies and acceptance following Eq. 2. The expected cross section for $Z \to \mu\mu$ decays as a function of statistics corresponding to different luminosity scenarios is also shown in Fig. 2. The results were normalized to the cross section determined with a MC sample corresponding to an integrated luminosity of 133 pb^{-1}. The expected statistical error at 10 pb^{-1} of integrated luminosity is about 2%. Both analyses showed similar sensitivities. The 10% luminosity uncertainty is again expected to dominate the total error.

6. Constraints to Parton Distribution Functions

The large W/Z cross sections at the LHC makes high-precision differential measurements possible. CMS performed a measurement of the muon differential cross section measurement as a function of muon pseudorapidity in inclusive $W \to \mu\nu$ production [14]. This analysis utilized the same trigger path as the inclusive $W \to \mu\nu$ cross section analysis. The $W \to \mu\nu$ candidates were selected with muon $p_T > 25$ GeV and MET>20 GeV. A calorimeter-based isolation was used to suppress the QCD dijet contribution. After correcting for efficiencies and acceptance, the ex-

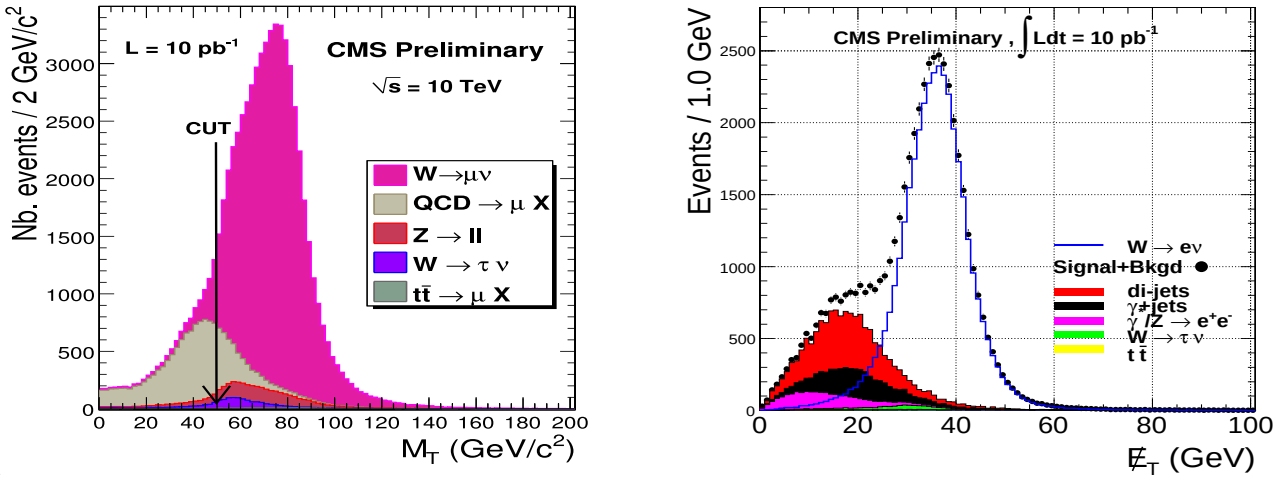

Figure 1: Left) The reconstructed $W \to \mu\nu$ transverse mass distribution. Right) The reconstructed $W \to e\nu$ MET distribution. Both are normalized to 10 pb^{-1} of integrated luminosity. The arrow in the left figure indicates that a cut on $m_T > 50$ GeV was applied to select final data sample.

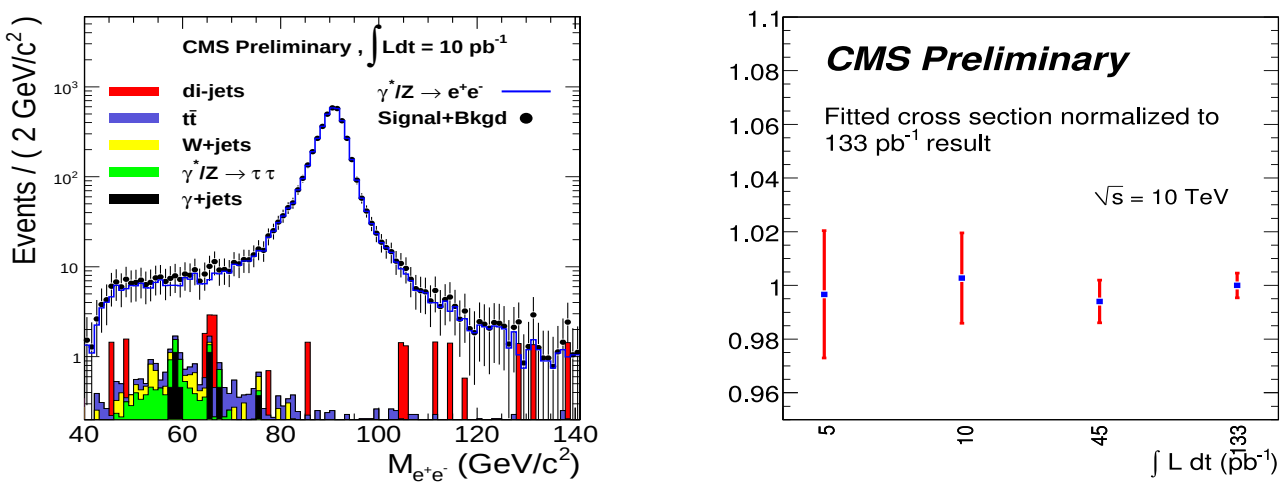

Figure 2: Left) The reconstructed $Z \to ee$ invariant mass distribution for an integrated luminosity of 10 pb^{-1}. Right) The $Z \to \mu\mu$ cross section as a function of MC statistics corresponding to different luminosity scenarios. The results were normalized to the cross section determined with 133 pb^{-1} of integrated luminosity. Only statistical errors are shown.

pected muon pseudorapidity distributions at an integrated luminosity of 10 pb^{-1} are shown in Fig. 3. The PDF error on the experimental data points is the theoretical error in estimating acceptance. Among other systematic errors, the 10% luminosity error dominates. The results were compared to theoretical predictions from Pythia. We estimated the PDF error using the CTEQ6M [15] PDF model with PDF-reweighting technique [16]. With 10 pb^{-1} of integrated luminosity, the results are still dominated by experimental systematic error.

To minimize experimental systematic errors, CMS also studied the muon charge asymmetry defined in Eq. 1 because many experimental errors cancel out. The PDF error on this quantity is only at few percent level [17]. The analysis strategy was identical to the muon differential cross section analysis described above. We computed the observed charge asymmetry, $A^{obs.}(\eta)$, with background subtracted number of $W \to \mu\nu$ signal events, $N^{W\to\mu\nu}(\eta)$,

$$A^{obs.}(\eta) = \frac{N^{W^+\to\mu^+\nu}(\eta) - N^{W^-\to\mu^-\nu}(\eta)}{N^{W^+\to\mu^+\nu}(\eta) + N^{W^-\to\mu^-\nu}(\eta)}, \qquad (3)$$

assuming that reconstruction and selection efficiency ratios between μ^+ and μ^- are one. Because of the weak decay of W bosons, the acceptance ratio between μ^+ and μ^- differs from unity. In this analysis, we did not correct for the acceptance difference in $A^{obs.}(\eta)$ but absorbed it into the theoretical predictions. The charge asymmetry as a function of muon pseudorapid-

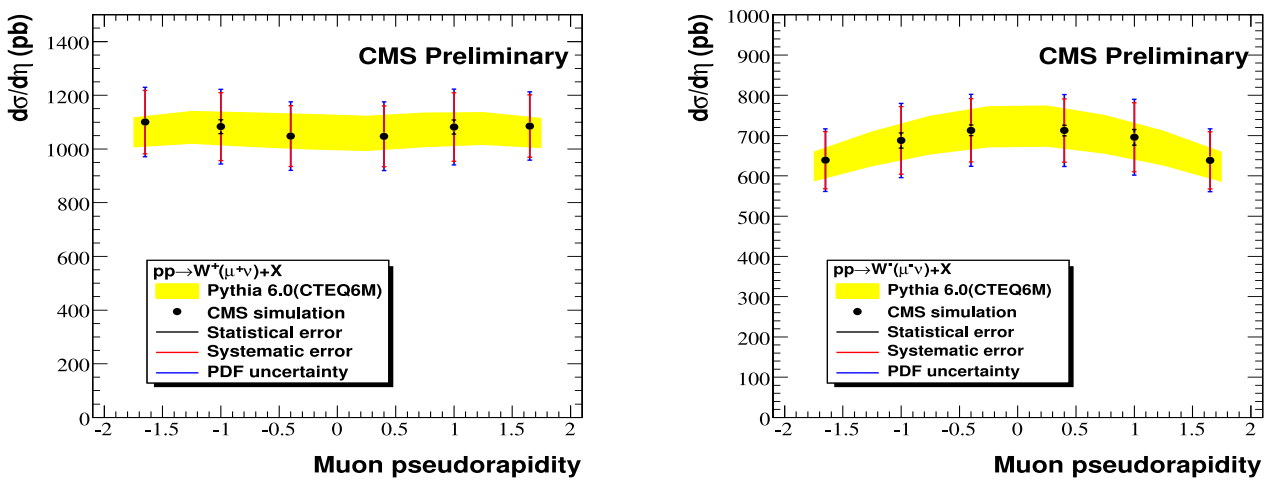

Figure 3: The expected $W \to \mu\nu$ differential cross sections for an integrated luminosity of 10 pb^{-1}. Left) μ^+, and Right) μ^-.

ity for an integrated luminosity of 100 pb^{-1} is shown in Fig. 4 [14]. The result is compared to theoretical predictions from Pythia, where the PDF error was estimated with CTEQ6M PDF model. The systematic error is dominated by the statistical error on the efficiency ratio between μ^+ and μ^- determined using 100 pb^{-1} of Drell-Yan MC. Even with a conservative treatment of systematic errors, the total errors of this measurement are comparable to the PDF errors and potentially could provide new constraints on different PDF models.

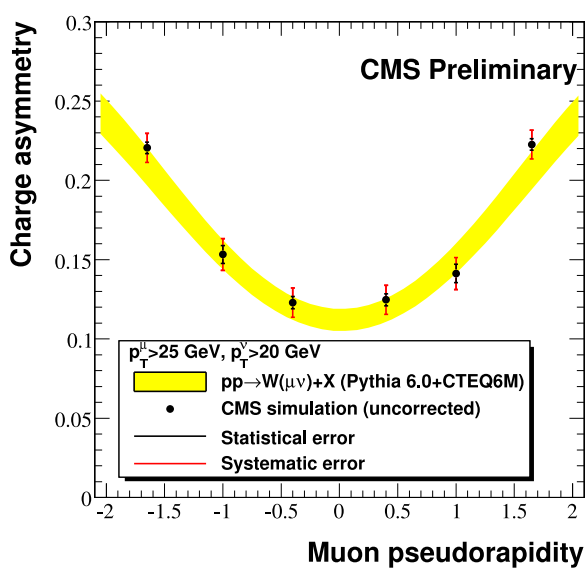

Figure 4: The expected muon charge asymmetry for 100 pb^{-1} of simulated luminosity. The systematic error is dominated by the statistical error on the efficiency ratio between μ^+ and μ^- determined using 100 pb^{-1} of Drell-Yan MC.

The Z boson differential cross section as a function of Z rapidity can also be used to test higher order perturbation calculations and put constraints on PDF models. CMS performed a study of this observable using $Z \to ee$ events [18]. To remove the luminosity uncertainty in this measurement, the following observable was studied,

$$\frac{1}{\sigma} \cdot \times \frac{d\sigma(Z \to ee)}{dy_i} = \frac{\sum_i (\epsilon \times A)_i}{\sum_i N_i} \cdot \frac{N_i}{\Delta_i (\epsilon \times A)_i}, \quad (4)$$

where for each bin i of rapidity (y_i), N_i is the number of background subtracted $Z \to ee$ candidates, Δ_i is the bin width, and $(\epsilon \times A)_i$ is the product of the efficiency and acceptance for detecting and reconstructing a Z boson with rapidity y_i.

With conventional electron reconstruction at the CMS, where both CMS ECAL and tracking system are utilized, the coverage for electrons is up to pseudorapidity of about 2.5. The reconstructed $Z \to ee$ candidates can be used to directly probe partons with kinematics [2] outside the range of previous experiments [4]. The kinematics reach was further extended by using electrons reconstructed using the CMS Forward Hadronic (HF) calorimeter [19], which has a coverage up to pseudorapidity of 4.6. The shower shape of HF reconstructed electron candidates was utilized to remove $Z \to ee$ background events effectively.

The final results for the rapidity measurement for an integrated luminosity of 100 pb^{-1} is shown in Fig. 5. The background in the HF region is well under control. The expected measurements are compared to

[2] Here the initial state parton momentum fraction $x_{1,2} = \frac{M_Z}{\sqrt{s}} \cdot e^{\pm y}$, where s is the center of mass energy at the LHC.

predictions with CTEQ6.1 PDF model [20]. With an integrated luminosity of 100 pb^{-1}, we are expecting to provide new constraints on different PDF models.

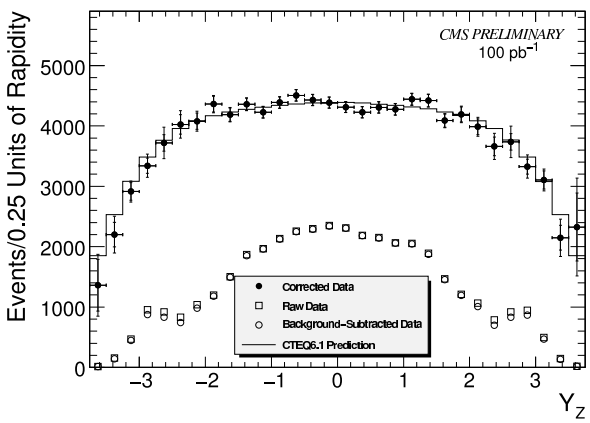

Figure 5: The expected Z boson rapidity shape for an integrated luminosity of 100 pb^{-1}.

7. Summary

CMS performed MC studies to explore W/Z boson production with initial LHC data. With 10 pb^{-1} of integrated luminosity, the inclusive W/Z cross sections could be established with 1-2% statistical precision. However, it is expected that the luminosity uncertainty will dominate the total error in these measurements.

The sensitivities to constrain different PDF models at CMS were also explored using measurements of the muon charge asymmetry in inclusive $W \to \mu\nu$ process and the Z rapidity shape in inclusive $Z \to ee$ process. With about 100 pb^{-1} of integrated luminosity, both measurements could provide constraints on different PDF models.

Acknowledgments

We thank the technical and administrative staff at CERN and other CMS Institutes, and acknowledge support from: FMSR (Austria); FNRS and FWO (Belgium); CNPq, CAPES, FAPERJ, and FAPESP (Brazil); MES (Bulgaria); CERN; CAS, MoST, and NSFC (China); COLCIENCIAS (Colombia); MSES (Croatia); RPF (Cyprus); Academy of Sciences and NICPB (Estonia); Academy of Finland, ME, and HIP (Finland); CEA and CNRS/IN2P3 (France); BMBF, DFG, and HGF (Germany); GSRT (Greece); OTKA and NKTH (Hungary); DAE and DST (India); IPM (Iran); SFI (Ireland); INFN (Italy); NRF (Korea); LAS (Lithuania); CINVESTAV, CONACYT, SEP, and UASLP-FAI (Mexico); PAEC (Pakistan); SCSR (Poland); FCT (Portugal); JINR (Armenia, Belarus, Georgia, Ukraine, Uzbekistan); MST and MAE (Russia); MSTDS (Serbia); MICINN and CPAN (Spain); Swiss Funding Agencies (Switzerland); NSC (Taipei); TUBITAK and TAEK (Turkey); STFC (United Kingdom); DOE and NSF (USA). Individuals have received support from the Marie-Curie IEF program (European Union); the Leventis Foundation; the A. P. Sloan Foundation; the Alexander von Humboldt Foundation.

References

[1] **UA2** Collaboration, M. Banner *et al.*, Phys. Lett. B **122**, 476 (1983).
[2] **UA1** Collaboration, G. Amison *et al.*, Phys. Lett. B **126**, 398 (1983).
[3] L. Evans *et al.*, JINST **3** S08001 (2008).
[4] J.M. Campbell, J.W. Huston, and W.J. Stirling, Rept. Prog. Phys. **70** 89 (2007).
[5] C. Anastasiou *et al.*, Phys. Rev. D **69**, 094008 (2004).
[6] **CMS** Collaboration, JINST **0803** S08004 (2008).
[7] T. Sjostrand *et al.*, Comput. Phys. Commun. **135** 2001.
[8] J. Pumplin *et al.*, arxiv:hep-ph/0201195.
[9] S. Agostinelli *et al.*, Nucl. Instrum. Methods. Phys. Res. A **506** 250 (2003).
[10] **CMS** Collaboration, CMS-PAS-EWK-09-001 (2009).
[11] **CMS** Collaboration, CMS-PAS-EWK-09-004 (2009).
[12] **CMS** Collaboration, CMS-PAS-EWK-07-002 (2007).
[13] H.Jung *et al.*, arxiv:hep-ph/0903.3861.
[14] **CMS** Collaboration, CMS-PAS-EWK-09-003 (2009).
[15] J. Pumplin *et al.*, JHEP **0207**, 12 (2002).
[16] D. Bourilkov, R. Group, and M. Whalley, arxiv:hep-ph/0605240v2.
[17] A.M. Cooper-Sarkar, talk in PDF4LHC workshop (2009).
[18] **CMS** Collaboration, CMS-PAS-EWK-09-005 (2009).
[19] G. Baiatian *et al.*, Eur. Phys. J. **C53** 139 (2008).
[20] S. Kretzer *et al.*, Phys. Rev. D. **69**, 114005 (2004).